Is Primate Lens Accommodation Unilaterally or Bilaterally Controlled?

Paul J. May[1–3] and Paul D. Gamlin[4]

[1]Department of Neurobiology and Anatomical Sciences, University of Mississippi Medical Center, Jackson, Mississippi, United States
[2]Department of Ophthalmology, University of Mississippi Medical Center, Jackson, Mississippi, United States
[3]Department of Neurology, University of Mississippi Medical Center, Jackson, Mississippi, United States
[4]Department of Ophthalmology and Visual Sciences, University of Alabama at Birmingham, Birmingham, Alabama, United States

Correspondence: Paul J. May, PhD, Department of Neurobiology & Anatomical Sciences, University of Mississippi Medical Center, 2500 North State Street, Jackson, MS 39216, USA;
pmay@umc.edu.

Received: April 9, 2020
Accepted: May 20, 2020
Published: July 7, 2020

Citation: May PJ, Gamlin PD. Is primate lens accommodation unilaterally or bilaterally controlled?. *Invest Ophthalmol Vis Sci.* 2020;61(8):5.
https://doi.org/10.1167/iovs.61.8.5

Purpose. In frontal-eyed mammals such as primates, eye movements are coordinated so that the lines of sight are directed at targets in a manner that adjusts for target distance. The lens of each eye must also be adjusted with respect to target distance to maintain precise focus. Whether the systems for controlling eye movements are monocularly or binocularly organized is currently a point of contention. We recently determined that the premotor neurons controlling the lens of one eye are bilaterally distributed in the midbrain. In this study, we examine whether this is due to premotor neurons projecting bilaterally to the preganglionic Edinger-Westphal nuclei, or by a mixture of ipsilaterally and contralaterally projecting cells supplying each nucleus.

Methods. The ciliary muscles of *Macaca fasicularis* monkeys were injected with recombinant forms of the N2c rabies virus, one eye with virus that produced a green fluorescent marker and the other eye with a virus that produced a red fluorescent marker.

Results. Preganglionic motoneurons in the Edinger-Westphal nucleus displayed the same marker as the ipsilateral injected muscle. Many of the premotor neurons in the supraoculomotor area and central mesencephalic reticular formation were doubly labeled. Others were labeled from either the ipsilateral or contralateral eye.

Conclusions. These results suggest that both monocular control and binocular control of lens accommodation are present. Binocular inputs yoke the accommodation in the two eyes. Monocular inputs may allow modification related to differences in each eye's target distance or differences in the capacities of the two ciliary muscles.

Keywords: Edinger-Westphal, vergence, near triad, oculomotor, saccade

Saccadic and smooth pursuit movements of the eyes directed at specific targets have generally been tested under conditions where they are conjugate in nature, and considered as separate from vergence movements used to look between targets at different distances from the viewer. However, under real-world circumstances, most new targets differ from the current foveation point in all three axes; that is, they require both a change in the line of sight, as well as a change in vergence angle. The viewer is thus required to make disjunctive saccadic or pursuit eye movements. In frontal-eyed species, such as higher primates, the actions of the extraocular and intraocular muscles are coordinated so that, in addition to modifying the vergence angle between the two eyes, the response also involves binocular changes in lens accommodation and pupil size to compensate for the target distance. To look at a near target, the eyes are converged, the curvature of the lens is increased through the actions of the ciliary muscle, and the pupil is constricted by the pupillary sphincter muscle to increase depth of field. This combination is commonly referred to as the near response or near triad.

The manner in which premotor neurons control the motoneuron population to match such three-axis target requirements has been a matter of dispute for more than a century. Hering[1] proposed that vergence eye movement signals related to target distance and conjugate eye movement signals related to the other aspects of target location are developed independently. These two binocularly organized signals are then added together at the level of the extraocular motoneurons to produce the appropriate movement of the two eyes. Helmholtz,[2] on the other hand, proposed that each eye was independently controlled, eliminating the need for separate signals for the target distance axis. In this case, monocular signals are used to direct the extraocular motoneuron populations. Evidence supporting both theories of eye movement has been developed. In support of Hering's view, centers containing premotor neurons for each axis have been described: a horizontal axis center in the paramedian pontine reticular formation (PPRF) and nucleus prepositus hypoglossi (nPH); a vertical axis center in the rostral interstitial nucleus of the medial longitudinal fasciculus and in the interstitial nucleus of Cajal;

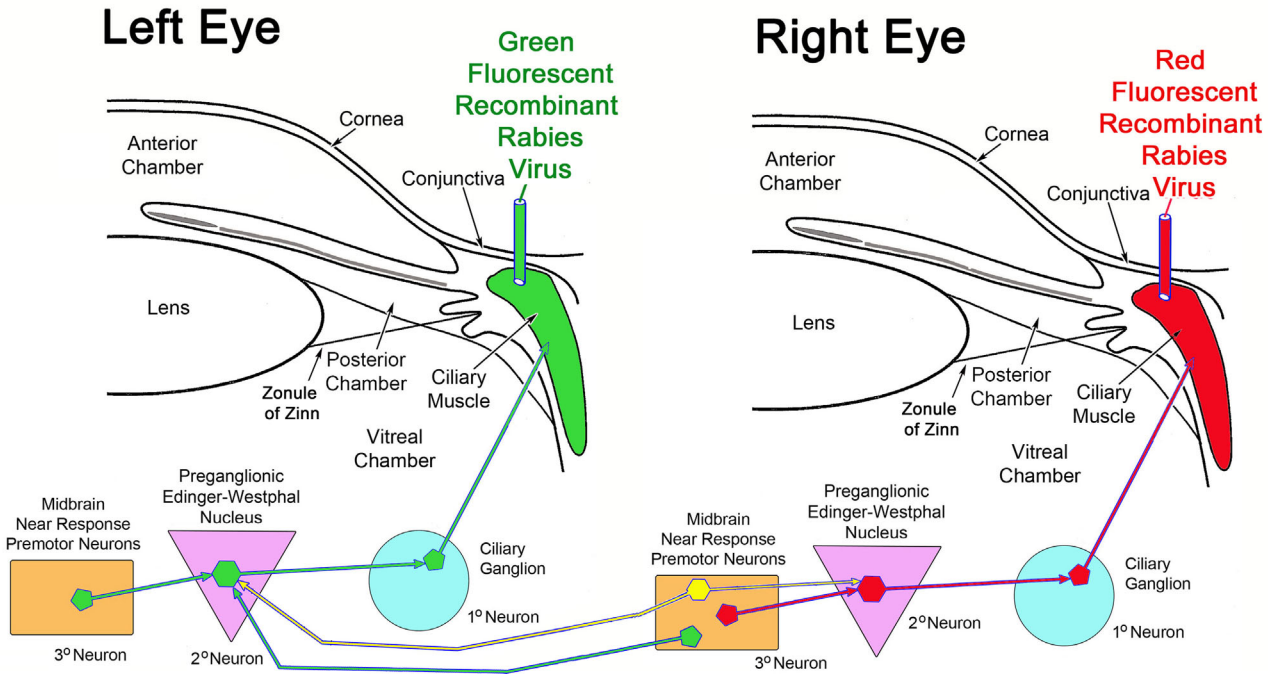

Figure 1. Schematic of double-label method. A green fluorescing recombinant rabies virus (N2c-GFP) is placed in the ciliary muscle on one side (left eye) and a red fluorescing recombinant rabies virus (N2c-mCherry) is placed in the ciliary muscle on the other side (right eye). Retrograde trans-synaptic transport to third-order neurons labels the premotor population. The premotor neurons can be labeled either from the left eye (*green*), right eye (*red*), or both eyes (*yellow*). To simplify the diagram, the individual possibilities are only illustrated once, even though they might occur on both sides.

and a distance or Z-axis center amongst the midbrain near response neurons.[3] In support of Helmholtz's theory, cells in the PPRF and in the nPH have been shown to be predominantly monocular in their organization.[4,5]

These discussions have largely centered on the control of horizontal eye movements. Little attention has been paid to other aspects of the near response that must be coordinated with vergence eye movements when making disjunctive eye movements to targets of different distances. However, most of the midbrain neurons that fire in a manner that encodes vergence angle also display activity that encodes lens accommodation, and these neurons are mixed with cells that encode predominantly vergence or lens accommodation.[6,7] We have recently identified the premotor cells that control lens accommodation anatomically, by using injections of the ciliary muscle with rabies virus, a trans-synaptic retrograde tracer.[8,9] The premotor neurons were located in the supraoculomotor area (SOA) and in the central mesencephalic reticular formation (cMRF). One of the striking characteristics of both these populations is that unilateral injections led to a balanced bilateral distribution of labeled neurons. Injections of anterograde tracer into the cMRF also produce terminal label bilaterally in the preganglionic Edinger-Westphal nucleus (EWpg).[10] Similarly, unilateral injections of rabies virus into the lateral rectus muscle of monkeys or the medial rectus muscle of guinea pigs produced bilateral SOA and cMRF labeling of premotor neurons,[11,12] and unilateral cMRF injections label terminals contacting motoneurons that supply multiply innervated fibers in the medial rectus muscle, bilaterally.[13]

The bilateral nature of all these labeled midbrain populations could be produced by two different means: (1) all the premotor neurons project bilaterally, targeting EWpg motoneurons and horizontal gaze somatic motoneurons on both sides of the brainstem; or (2) ipsilaterally and contralaterally projecting premotor neurons are intermixed. An examination of this question could have implications for discriminating between the binocular control theory of Hering and the monocular control theory of Helmholtz. Consequently, we have used trans-synaptic retrograde transport of recombinant rabies virus to examine this point.

Methods

A total of four adult and young adult female *Macaca fascicularis* monkeys were used in these experiments. The surgical procedures were approved by the Institutional Animal Care and Use Committee of the University of Pittsburgh, and were in full accordance with those outlined by the Guide for Care and Use of Animals and the ARVO Statement for the Use of Animals in Ophthalmic and Vision Research. Before the injection procedures were carried out, the animals were sedated with ketamine HCl (10–15 mg/kg, IM) and then placed under general anesthesia by use of isoflurane (3.0% in O_2). Ophthalmic proparacaine drops were placed in each eye. Animals received buprenorphine HCl (0.01 mg/kg, IM) as a postoperative analgesic at the conclusion of the procedure.

The experimental rationale is illustrated in Figure 1. The ciliary muscle of one eye (e.g., left) was injected with a recombinant rabies virus that produces a green fluorescent protein (GFP) marker. The ciliary muscle of the other eye (e.g., right) was injected with a recombinant rabies virus that produces a red fluorescent marker (mCherry).

Investigative Ophthalmology & Visual Science

Both recombinant viruses were taken up by postganglionic parasympathetic fibers and transported back to their cell bodies in their respective ciliary ganglia. After replication there, they crossed the synapse and were taken up by the axons of preganglionic parasympathetic motoneurons. Retrograde transport brought them to the ipsilateral EWpg. Consequently, after replication, they would fluoresce with the marker injected into the ipsilateral muscle. The virus then crossed the synapse into the terminals of the premotor neurons, and was taken up and retrogradely transported by their axons to their somata. After replication, those premotor neurons supplying the left EWpg would fluoresce green, those supplying the right EWpg would fluoresce red, and any cells supplying both EWpg nuclei would fluoresce with both markers, and so appear yellow/orange in the merged image.

All surgeries, postoperative survivals, and perfusions took place at the Center for Neuroanatomy with Neurotropic Viruses at the University of Pittsburgh directed by Dr Peter L. Strick. In each case, the ciliary muscle of one eye was injected with 150 µL of a solution containing 1×10^9 Pfu/mL of a recombinant N2c rabies virus that produces GFP (N2c-GFP). The ciliary muscle of the other eye was injected with 150 µL of a solution containing 1×10^9 Pfu/mL of a recombinant N2c rabies virus that produces a red fluorescent protein, mCherry (N2c-mCherry). These recombinant viruses were developed by Drs Matthias Schnell and Christoph Wirblich of Thomas Jefferson University. The virus was held in a 100-µL Hamilton syringe equipped with a 25G needle. Multiple (12–15) small (~10 µL) injections were made at different locations on the globe by driving the needle through the sclera at the corneal/conjuctival junction. The medial and ventromedial aspect of the ciliary body could not be accessed. Animals survived for 72 ($n = 1$), 76 ($n = 1$), and 80 hours ($n = 2$). They were then resedated with ketamine and deeply anesthetized with sodium pentobarbital (40 mg/kg, IP). Once insensate, they underwent a cardiac perfusion with phosphate buffered (0.1 M, pH 7.4) saline, followed by 10% formalin in phosphate buffer (0.1M, pH 7.4), and followed in turn by buffered formalin containing 5% glycerol. The brains were blocked in the frontal plane and post-fixed in a 10% glycerol-buffered formalin solution for 7 days at 4°C. Several ganglia (ciliary, trigeminal, pterygopalatine, and superior cervical) were also extracted and processed to test for the presence of rabies virus (for details[8]). Of these, only the ciliary ganglia contained labeled cells, indicating that uptake by other postganglionic motoneurons supplying the eye did not occur.

The brainstems of these animals were frozen and cut into 50 µm thick sections. Every fifth section was reacted to reveal the presence of the two markers using antibodies to GFP (goat polyclonal antibody: Abcam # 5450; Abcam, Cambridge, UK) and to DsRed, which cross-reacts with mCherry (rabbit polyclonal antibody: Clonetech # 632496; Clonetech, Mountain View, CA). Specifically, sections were first rinsed in 0.1 M, pH 7.5 phosphate tris-buffered saline with 0.05% sodium azide (PTA). They were then placed in immunoblocking serum consisting of 10% normal donkey serum in PTA with 0.5% Triton-X 100 for 2 hours. They were incubated in a primary antibody solution consisting of 1:200 goat anti-GFP (Novus Biologicals # NB100-1770; Novus Biologicals, Littleton, CO) and 1:1000 rabbit anti-DsRed (TaKaRa #632496; TaKaRa, Mountain View, CA) in PTA with 10% normal donkey serum and Triton-X 100 for 2 days at 4°C with gentle agitation. After rinsing, the primary antibodies were subsequently tagged with fluorescent secondary antibodies: donkey anti-goat IgG conjugated to green fluorescing Alexa Fluor 488 (Jackson ImmunoResearch # 705-545-147; Jackson ImmunoResearch, West Grove, PA) and donkey anti-rabbit IgG conjugated to red fluorescing Alexa Fluor 594 (Jackson ImmunoResearch # 711-585-152). These were diluted 1:300 and 1:500, respectively, in a solution of PTA with 10% normal donkey serum and 0.3% triton-X-100. After incubating for 2 hours at room temperature in the secondary antibody solution, the sections were rinsed and mounted onto glass slides. Once they had dried, they were coverslipped under nonfluorescing medium. Control sections in which the primary or secondary antibody was omitted were run and they showed very weak or no fluorescence.

An adjacent series of sections was mounted onto glass slides, counterstained with cresyl violet, dehydrated, cleared, and coverslipped to provide a cytoarchitectonic context for the location of fluorescent-labeled cells. To measure the effectiveness of the labeling with the recombinant viruses and fluorescence procedures, another series was incubated in a mouse monoclonal antibody to the rabies virus (diluted 1:1000) as the primary antibody. (This was a gift of Dr Matthias Schnell of Thomas Jefferson University [designated clone 31G10]). The primary antibody was tagged with biotinylated anti-mouse IgG and revealed using a Vector Labs ABC kit (Vector Labs, Burlingame, CA), followed by DAB immunohistochemistry. The details of this procedure can be found in our previous study.[8]

Sections were analyzed by use of a Nikon E600 fluorescence photomicroscope equipped with a Nikon Ds-Ri1 digital camera. Nikon Elements software was used to import the images into the computer. Image contrast and brightness were adjusted in Photoshop to appear as similar as possible to the viewed image. Color prints of the images were used to create chartings of the label, with borders supplied by comparison with adjacent Nissl-stained sections. In each case, we used prints of the images obtained with the filters for the mCherry (TRITC excitation bandwidth 525–553) and the GFP marker (FITC excitation bandwidth 465–495). These images were compared with the merged image to make sure singly and doubly labeled neurons were correctly identified. In addition, we consulted an image taken with the filters for blue fluorescent markers (UV excitation bandwidth 330–380) to ensure that the cells were not simply fluorescing due to the presence of lipofuscin or other nonspecific labeling.

Results

The results from the 72-hour survival animal are presented in Figure 2. This animal was not useful with respect to the bilateral labeling question because we had insufficient labeling from the left eye injection (blue dots), with only a handful of cells labeled (Figs. 2A, 2D). However, it was useful in establishing the lower limit of survival time for trans-synaptic transport to the premotor population. Most of the retrograde trans-synaptic labeling from an injection of the right eye (red diamonds) was found in the motoneurons located in the right EWpg (Figs. 2B–2I) and right anteromedian nucleus (Fig. 2A). Just a handful of neurons were found at sites known to contain premotor neurons, including the SOA (Figs. 2D, 2E, 2G, 2I), and in the peri-interstitial nucleus of Cajal portion of the mesencephalic reticular formation (Figs. 2C, 2D). Based on our previous findings, the two cells located between the oculomotor nuclei (III) (Fig. 2B) might be either motoneurons or premotor neurons.[8]

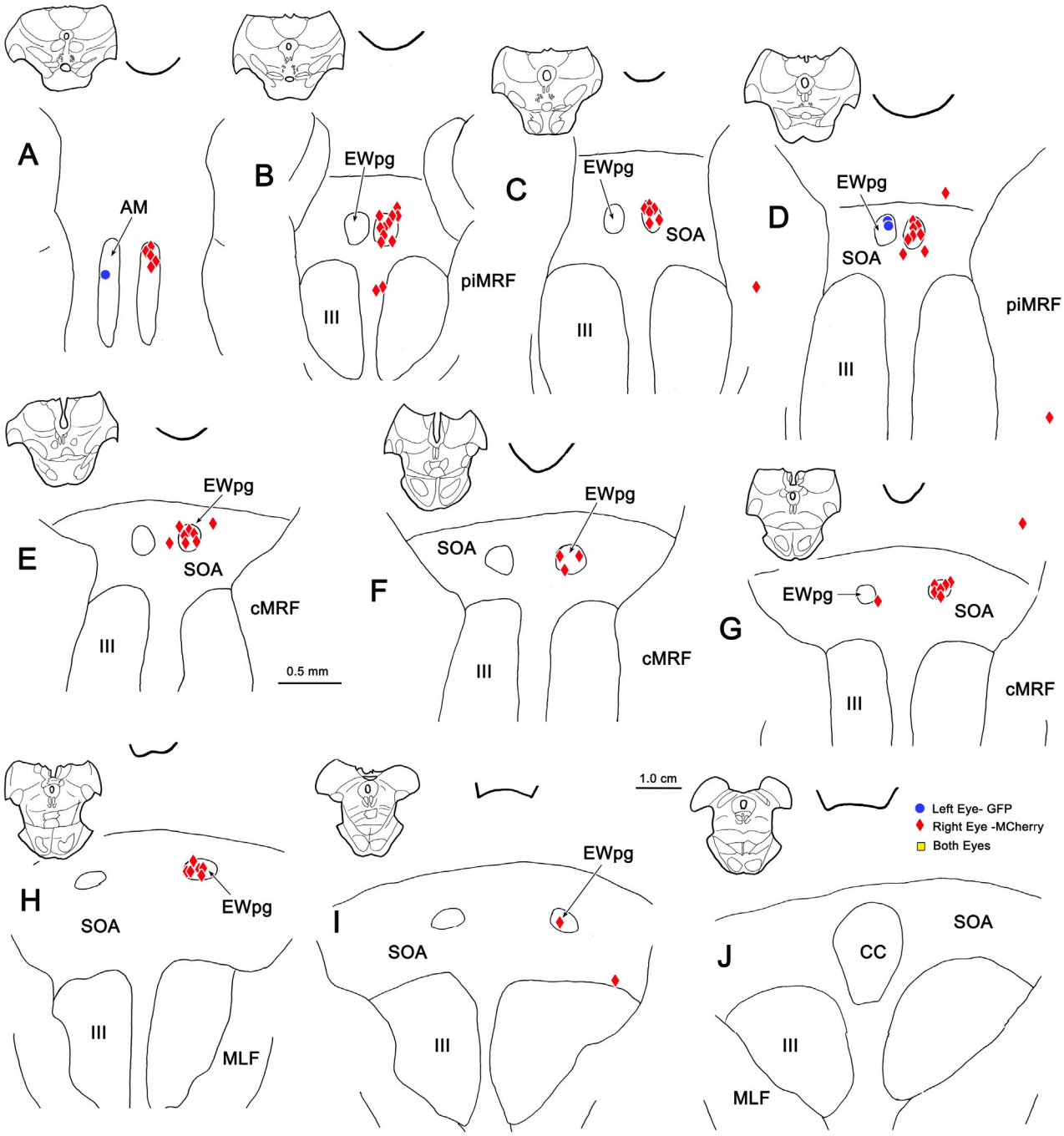

Figure 2. Distribution of retrograde, fluorescent trans-synaptic label after a 72-hour survival period. Chartings of a rostral to caudal series through the region containing the AM (**A**) and EWpg (**B–I**) show the distribution of cells labeled from the left (*blue dots*) and right (*red diamonds*) ciliary muscle injections. The left injection was not effective, and only a few labeled motoneurons were present in the ipsilateral EWpg in sections **A** and **D**. Numerous motoneurons were observed in the ipsilateral AM and EWpg from the injection on the right side. The presence of just a few labeled neurons outside these nuclei indicates that transfer of virus to premotor neurons had just begun at this time point. Inserts indicate the section from which the higher magnification drawing was made in this and the following chartings. 3n, third cranial nerve; AM, anteromedian nucleus; CC, caudal central subdivision of III; CG, central gray; III, oculomotor nucleus; MLF, medial longitudinal fasciculus; PAG, periaqueductal gray; piMRF, peri-interstitial nucleus of Cajal portion of the mesencephalic reticular formation.

Many more labeled premotor neurons were observed at 76 hours. Examples of the SOA premotor neurons labeled in a case with a 76-hour survival are presented in Figure 3A and 3B. GFP marker is present in neurons (green arrows) in both the left SOA (Fig. $3A_1$) and the right SOA (Fig. $3B_1$). The mCherry marker is also present in neurons (red arrows) in both the left SOA (Fig. $3A_2$) and the right SOA (Fig. $3B_2$). The merged images show that many of the neurons in the left SOA (Fig. $3A_3$) and the right SOA (Fig. $3B_3$) are double labeled and so display a yellow or orange tint (yellow

Investigative Ophthalmology & Visual Science

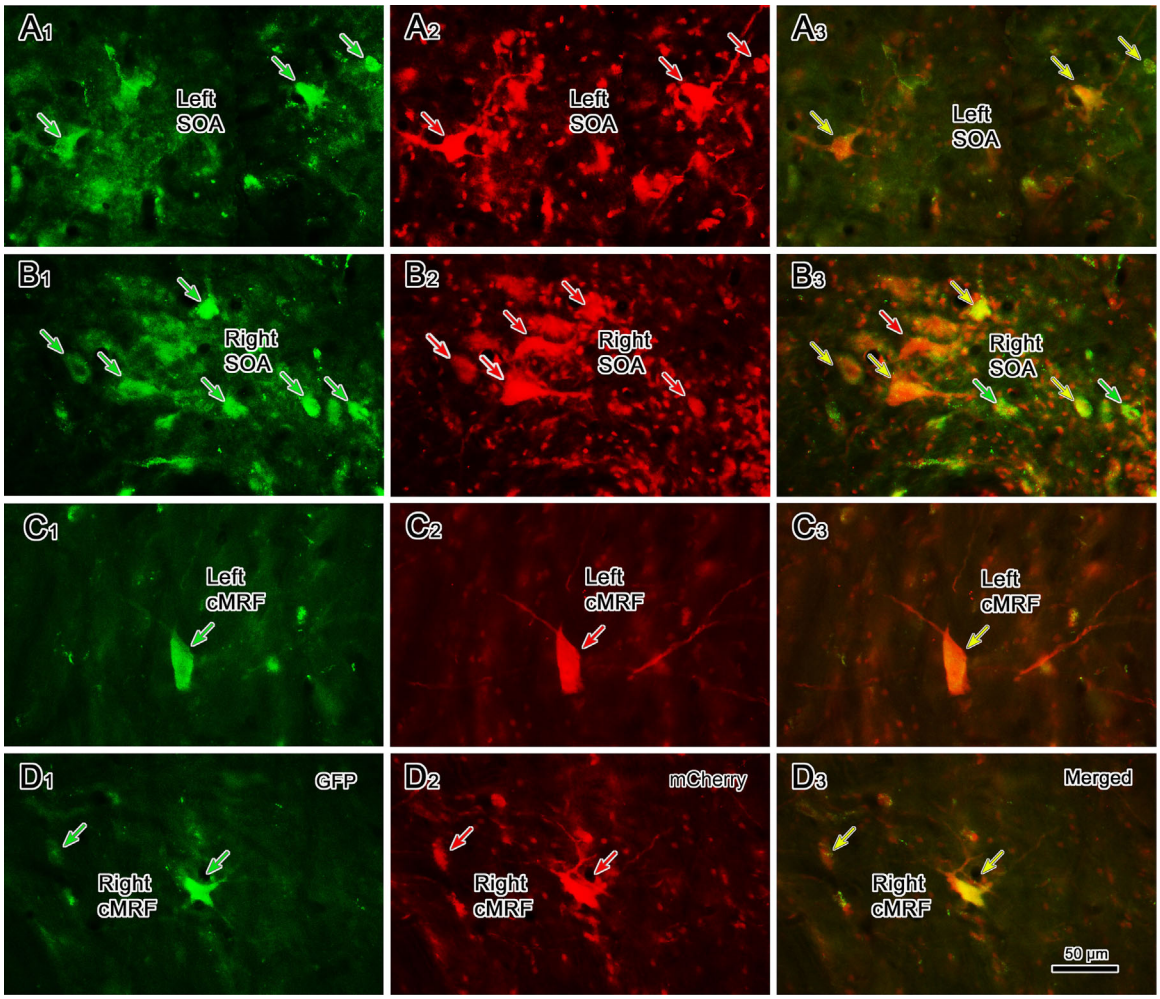

Figure 3. Appearance of singly and doubly labeled premotor neurons at 76 hours. Fluorescent labeling in the left (**A**) and right (**B**) SOA, and in the left (**C**) and right (**D**) cMRF shows both singly and doubly labeled neurons. The appearance of the same sections is shown to demonstrate GFP labeling in the left column, mCherry labeling in the middle column, and the merged image in the right column. Cells labeled with GFP are indicated by *green arrows*, those with mCherry labeling by *red arrows*. Those with both markers in the merged view are indicated by *yellow arrows*. Scale in **D3** is for all plates.

arrows). However, a few show just the GFP marker from the left eye (green arrows) or just the mCherry from the right eye (red arrow). If we could not make out the outlines of a neuron in one of the individual filter images, we judged the cell to be single labeled, even if it had an orange color in the merged image (red arrow, Figs. 3B$_1$–3B$_3$).

With a survival time that was just 4 hours longer than the case illustrated in Figure 2, the 76-hour case showed a very different labeling pattern. As demonstrated in Figure 4, in this case there was good uptake from both eyes. Numerous preganglionic motoneurons were labeled rostrally in anteromedian nucleus (Fig. 4A) and more caudally in EWpg (Figs. 4B–4G). Cells labeled from the left eye (blue dots) and cells labeled from the right eye (red diamonds) populate both these nuclei ipsilaterally. Within the SOA (Figs. 4A–4I) numerous doubly labeled neurons (yellow squares) were observed on both sides of the midline. These were particularly prevalent caudally (Figs. 4H, 4I). Neurons that only showed tracer from the left eye (blue dots) were also present bilaterally in the SOA, as were cells that just showed tracer from the right eye (red diamonds). So, all three patterns of labeling were present bilaterally and were more common at caudal levels. A few cells that are presumed to be premotor neurons were found within the confines of EWpg (yellow squares in Fig. 4E and blue dot in Fig. 4G). Examples of scattered premotor labeling within the borders of the contralateral EWpg were observed previously with conventional rabies virus labeling.[8]

Areas outside the SOA also contained labeled premotor neurons in this case. The distributions of labeled premotor neurons within the cMRF are presented in Figures 5 and 6. On the left side (Fig. 5), the labeled motoneurons present in the EWpg were only from the left eye injection (blue dots) (Figs. 5A–5H). However, at rostral levels (Figs. 5A–5E), all three labeling patterns were seen among the premotor neurons that lay amongst the exiting oculomotor nerve (3n) bundles: cells labeled from the left eye (blue dots), right eye (red diamonds) and from both sides (yellow squares). At more caudal levels (Figs. 5F–5I), the premotor neurons formed a band across the left cMRF. There, the double labeled neurons predominated, but cells labeled from just the ipsilateral and contralateral eye were also present. An example of such a double labeled cell in the left cMRF is shown in Figure 3C. On the right side (Fig. 6),

Investigative Ophthalmology & Visual Science

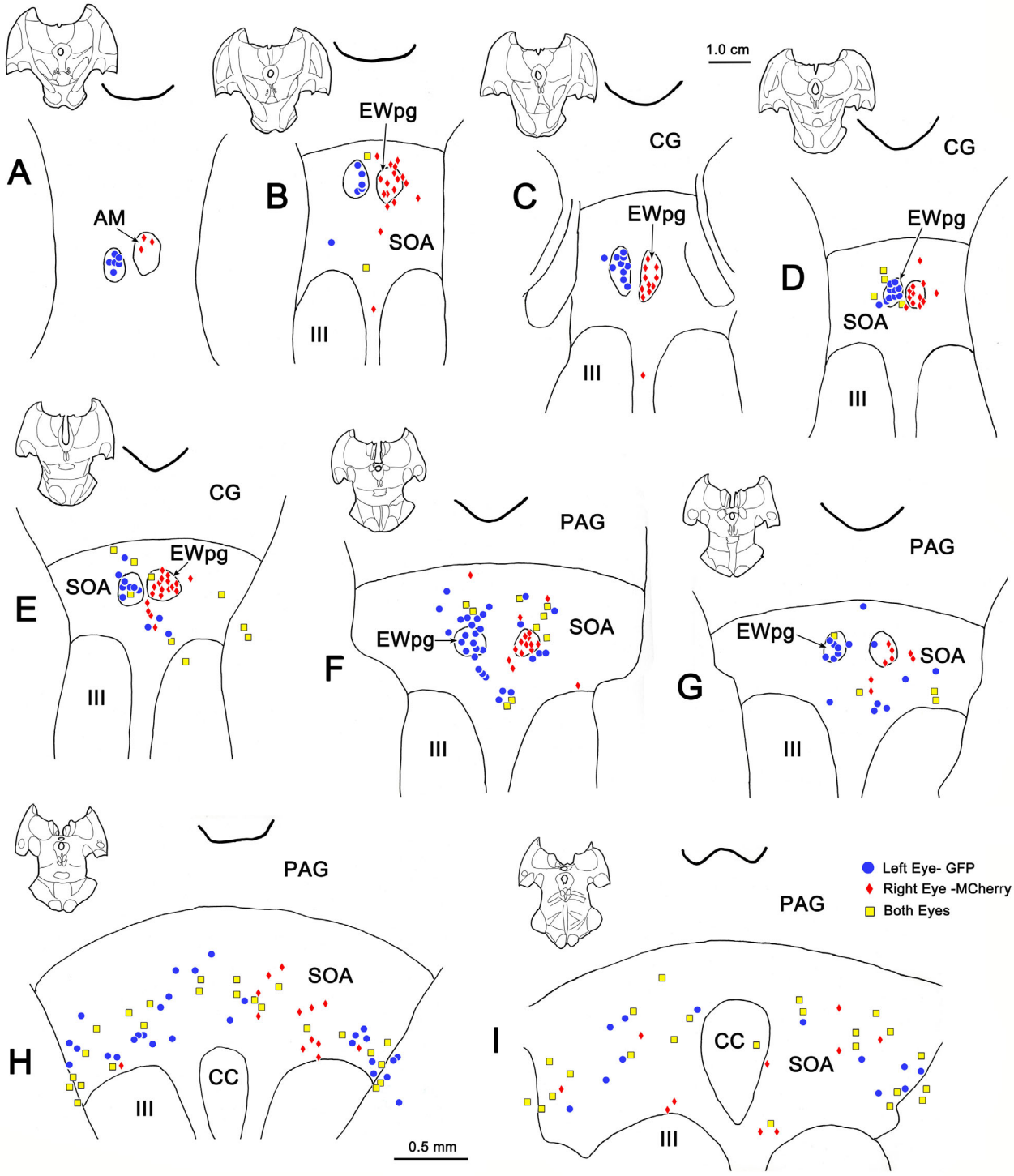

Figure 4. Distribution of retrograde, fluorescent trans-synaptic label in the SOA after a 76-hour survival period. Chartings of a rostral to caudal series through the region show the distribution of cells labeled from the left (*blue dots*) and right (*red diamonds*) ciliary muscle injections. Numerous motoneurons were labeled in the left AM (**A**) and EWpg (**B–H**) with the tracer injected into the left ciliary muscle, and in the right AM and EWpg with the tracer injected into the right ciliary muscle. Labeled premotor neurons were found in the SOA (**B–I**), particularly caudally. These included singly labeled cells both ipsilateral and contralateral to the injections, as well as many doubly labeled neurons (*yellow squares*).

the labeled motoneurons present in the EWpg were only from the right eye (red diamonds) (Figs. 6A–6H). However, at rostral levels (Figs. 6A–6E), all three labeling patterns were seen among the scattered premotor neurons adjacent to the exiting 3n bundles and in the peri-intestinal portion of the mesencephalic reticular formation: cells labeled from the left eye (blue dots), right eye (red diamonds) and from both sides (yellow squares). At more caudal levels

Investigative Ophthalmology & Visual Science

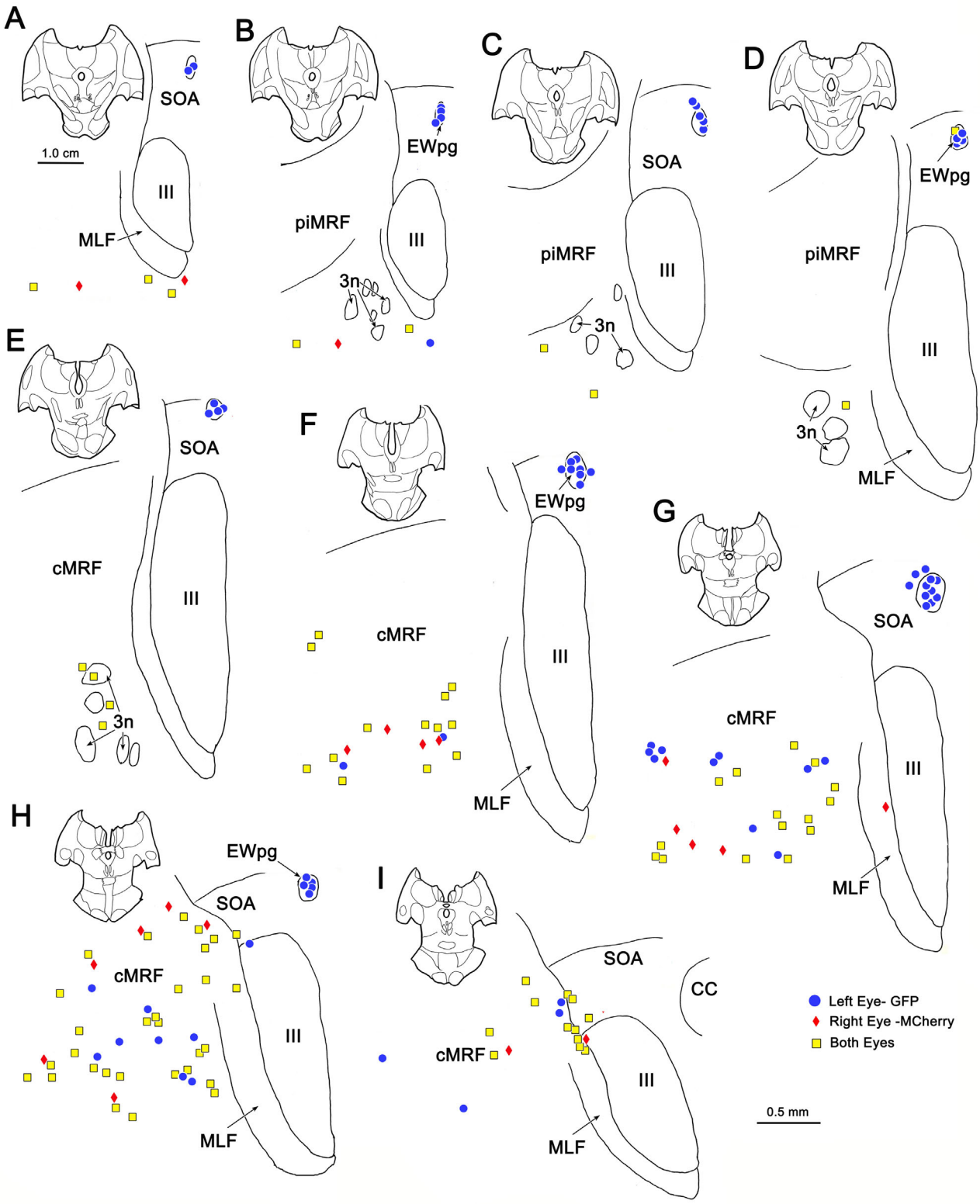

Figure 5. Distribution of retrograde, fluorescent trans-synaptic label in the left cMRF after a 76-hour survival period. Chartings of a rostral to caudal series through the region show the distribution of cells labeled from the left (*blue dots*) and right (*red diamonds*) ciliary muscle injections, as well as doubly labeled neurons (*yellow squares*). Labeled motoneurons from the left ciliary muscle injection lie in the ipsilateral EWpg (**A**–**H**). A few labeled premotor neurons were found amongst the exiting 3n fibers (**A**–**E**) and numerous labeled premotor neurons were located in the left cMRF (**F**–**I**). Most were double labeled neurons, although both ipsilateral and contralateral singly labeled neurons were present. SOA labeling is not shown.

Investigative Ophthalmology & Visual Science

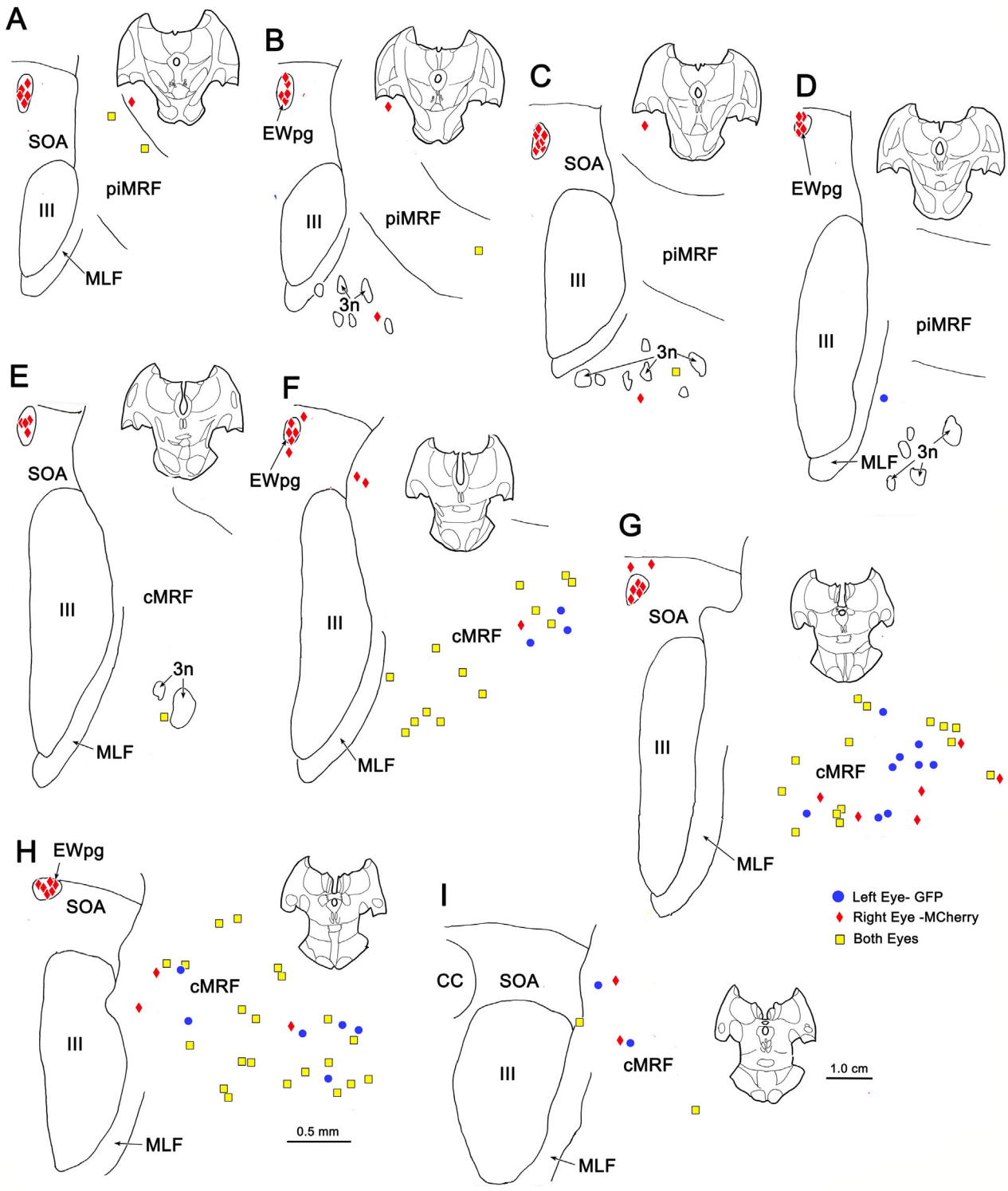

Figure 6. Distribution of retrograde, fluorescent trans-synaptic label in the right cMRF after a 76-hour survival period. Chartings of a rostral to caudal series through the region show the distribution of cells labeled from the left (*blue dots*) and right (*red diamonds*) ciliary muscle injections, as well as doubly labeled neurons (*yellow squares*). Labeled motoneurons from the right ciliary muscle injection lie in the ipsilateral EWpg (**A–H**). A few labeled premotor neurons were found in the peri-interstitial portion of the mesencephalic reticular formation (piMRF) (**A–C**) and amongst the exiting 3n fibers (**B–E**). Most of the labeled premotor neurons were located in the cMRF (**F–I**). The majority of these were double-labeled neurons. SOA labeling is not shown.

Investigative Ophthalmology & Visual Science

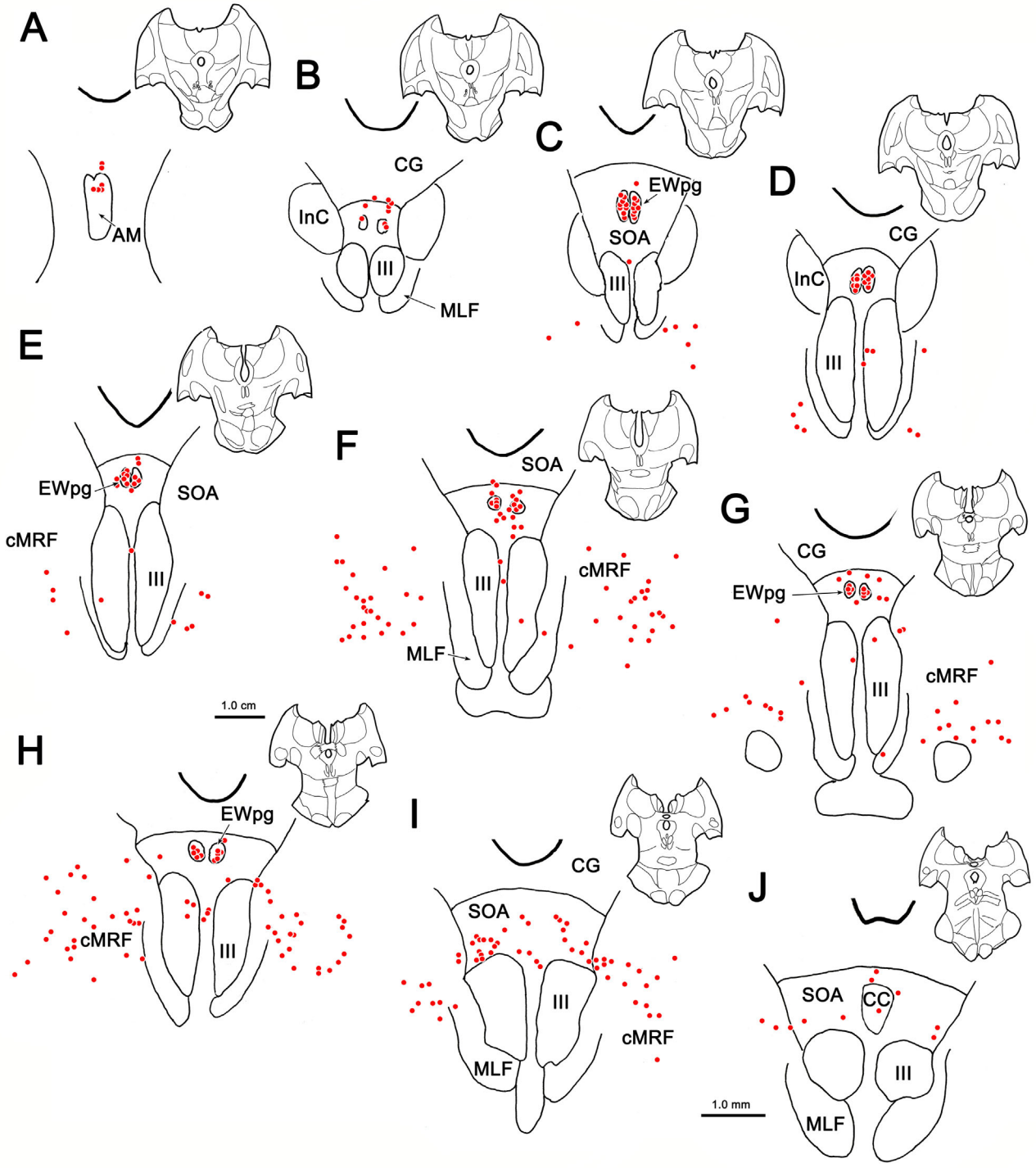

Figure 7. Distribution of trans-synaptically transported rabies virus after a 76-hour survival period. Chartings of a rostral to caudal series (**A–J**) through the region show the distribution of cells visualized using anti-rabies antibody (*red dots*). The pattern and number of labeled cells in the EWpg, SOA, and cMRF is very similar to that seen using the fluorescence methods.

(Figs. 6F–6I), the premotor neurons formed a band across the right cMRF. Again, the double-labeled neurons predominated, but cells labeled from just the ipsilateral (red diamonds) and contralateral (blue dots) eye were also present. Examples of such double-labeled cells in the right cMRF are shown in Figure 3D.

To ensure that the recombinant viruses and fluorescence procedures were revealing the full extent of the premotor population, we reacted a series of sections from this 76-hour case using anti-rabies IgG with DAB as the chromagen. The results for this approach are shown in Figure 7. Labeled preganglionic motoneurons are present in the dorsal part of anteromedian nucleus (Fig. 7A) and throughout EWpg (Figs. 7B–7H). Labeled premotor neurons were present in the SOA, particularly caudally (Fig. 7B–7J). They were also present ventrolateral to the MLF, rostrally (Figs. 7C

Investigative Ophthalmology & Visual Science

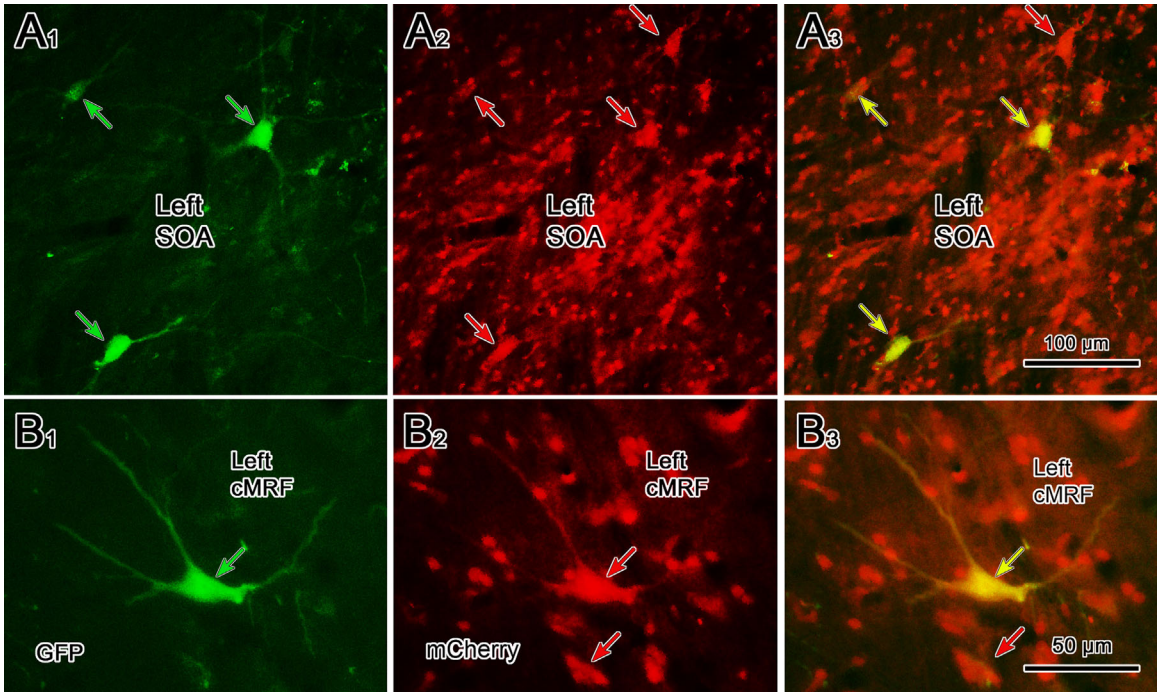

Figure 8. Appearance of singly and doubly labeled premotor neurons at 80 hours. Fluorescent labeling in the left (**A**) SOA and in the left (**B**) cMRF shows considerable dendritic labeling in both singly and doubly labeled neurons. The appearance of the same sections is shown to demonstrate GFP labeling in the left column, mCherry labeling in the middle column and the merged image in the right column. Cells labeled with GFP are indicated by green arrows, and those with mCherry labeling by red arrows. Those with both markers in the merged view are indicated by *yellow arrows*. Scale in $A_3 = A_1$ and A_2 and in $B_3 = B_1$ and B_2.

and 7D), and throughout the cMRF (Figs. 7E–7I). All these populations were labeled on both sides of the midline after injections of the ciliary body in both eyes. This distribution is very similar to that seen previously[8,9] and there are only a few more cells observable using this method than with the fluorescence labeling (Figs. 4–6).

The distributions of doubly and singly labeled neurons observed in the SOA and cMRF with the 80-hour survival period were much the same as with the 76-hour survival period. The primary difference observed was in the extent of the labeling. The GFP marker (green arrows) extended well out into the secondary dendrites in both the SOA cells (Fig. 8A_1) and in the cMRF cells (Fig. 8B_1). In some cases, mCherry (red arrows) also extended out into the secondary dendrites (Fig. 8B_2). As shown in the merged views, most of the cells in the SOA (Fig. 8A_3) and in the cMRF (Fig. 8B_3) were double labeled (yellow arrows), but some were just singly labeled (red arrows). Note that the cell indicated in the upper right (red arrow, Fig. 8A_2), also seems to have light label in the green filter (Fig. 8A_1). However, this fine particulate label also fluoresced with the blue filter, indicating the fine particulate labeling was lipofuscin. For this reason, the cell was judged to be singly labeled. The 80-hour time point is 8 hours later than the 72-hour time point, when just a few premotor neurons were labeled. So it is likely that inputs to these initially labeled premotor neurons would be starting to be observed at other sites. However, we did not analyze other regions, because this was beyond the purview of our experimental question.

Discussion

These results represent the first anatomic investigation of the laterality of the premotor control of lens accommodation. They show that most of the premotor neurons located in the SOA and the cMRF project bilaterally to the motoneurons in the EWpg. Thus, the majority of the input controlling lens accommodation to focus targets on the retinas of the two eyes is yoked. In addition, singly labeled neurons were observed in the SOA and cMRF that were either ipsilateral or contralateral to the eye they control the focus of (see premotor neuron box in Fig. 1). This finding suggests that the system may also have the capacity to monocularly modulate ciliary muscle activity, to independently adjust the degree of lens accommodation in each eye.

Technical Considerations

Recombinant viruses that produce different fluorescent tags have been used successfully in studies of this type.[14,15] Although only a small number of animals was used for each of the survival time points in the present study, the pattern of labeling in the midbrain was essentially the same as that seen in previous studies using the nonrecombinant N2c strain of rabies virus.[8,9] This finding suggests that the capacity of the recombinant virus to infect these motoneurons and transfer across synapses was not affected in the recombinant virus. The specificity of motoneuron uptake was also not changed. As with the normal virus, we saw no evidence of labeling in the superior cervical ganglion or thoracic spinal

Investigative Ophthalmology & Visual Science

cord indicating uptake by sympathetic fibers. Furthermore, we did not see labeling in the olivary pretectal nucleus that would indicate uptake by postganglionic parasympathetic fibers supplying the pupillary sphincter muscle. The presence of only ipsilateral labeling of EWpg in the case with the shortest survival time (72 hours), indicates that crossed projections by preganglionic motoneurons are not a factor. Only at the longest survival time did we see evidence of activated glial cells in EWpg. However, even at this time point, the motoneurons were intact, so nonsynaptic viral transfer is unlikely.

False-positive double labeling can be produced by high background labeling or lipofuscin deposits. We dealt with these problems by also viewing the tissue with the UVA filter set. Any cells that showed a similar degree of fluorescence with all three filter sets was judged to have nonspecific fluorescence, as opposed to the fluorescent markers tied to the specific labeling. The fact that the pattern of distribution of the labeled cells matches that using conventional rabies transport indicates that the singly labeled cells are unlikely to be false positives. It is possible that some of the singly labeled cells might actually project to both EWpg nuclei. We were unable to inject a portion of the ciliary muscle and some of the EWpg motoneurons were not labeled. Thus, it remains possible that some of the singly labeled premotor cells may provide input to motoneurons that were not labeled by the other tracer, making them a false negative with respect to double labeling. This point, and the small number of animals used in the study, made us conclude that it would be inappropriate to quantify the numbers of the doubly and singly labeled cells. Although many cells were double labeled, it should be noted that level of label from each side was not necessarily matched. Often, one of the labels was much more intense. This phenomenon may be due to the fact that, once a cell is infected by one recombinant rabies virus, it becomes resistant to being infected by the other rabies virus. Alternatively, it may be due to the fact that the number of ipsilateral and contralateral terminals produced by bilaterally projecting cells is not the same. One might argue that such unequal innervation might support a modified form of monocular control of accommodation. However, both sides would still be driven by premotor input, and setting up such a complex system for monocular control would represent a substantial developmental challenge.

Comparison With Previous Studies

As noted elsewhere in this article, the distribution of premotor neurons observed with the recombinant rabies virus matched that observed when conventional rabies virus was injected into the ciliary muscle.[8,9] These neurons were located in the SOA, especially caudally, and in the cMRF. These two regions also contain premotor neurons that supply the medial and lateral rectus muscles.[11,12] Physiologic studies indicate that the SOA contains midbrain near response neurons whose tonic firing encodes vergence angle,[7,16] and these cells even encode the inappropriate vergence angle seen in strabismus.[17–19] Many of these neurons encode both vergence and lens accommodation, although lens-only neurons are also present, as are neurons that just encode vergence angle.[6,7] So the neurons labeled in the SOA likely represent a combination of the first two.

The cMRF has also been shown to project bilaterally to the EWpg[10] and to the SOA,[20] where most of the dendrites of preganglionic motoneurons are located.[8] Premotor neurons in the cMRF also project bilaterally to motoneurons supplying medial rectus multiply innervated fibers, but ipsilaterally to motoneurons supplying singly innervated fibers in the same muscle.[13] Physiologic studies indicate the cMRF contains a very medially located population of vergence burst neurons that encode changes in intraocular angle during symmetric vergence movements.[21] It also contains more laterally located neurons that fire when disjunctive saccades are made.[22] Many of these neurons seem to encode the movement of only one of the eyes in their firing. A third population has recently been described.[23] These cells burst for disjunctive saccades, but not for conjugate saccades or symmetric vergence movements. Based on the numerous premotor neurons found in the cMRF after ciliary muscle injections[9] (present data), it seems highly likely that these three populations contain neurons that also direct lens accommodation with respect to target distance to focus the eye on the target, even as the line of sight is being adjusted with respect to target location.[7] However, this point remains to be addressed experimentally.

Laterality

Two theoretical frameworks have been proposed to explain the control of the eye with respect to target location in three-dimensional space. The Hering model[1] proposes that all horizontal eye movements can be explained by combining a conjugate movement signal that moves the eyes with respect to target location in the *X–Y* plane, and a symmetric vergence signal that moves the two eyes with respect to target distance. In contrast, the Helmholtz model[2] proposes that each eye is independently directed at the target, and so there is no need to separately direct the eyes with respect to target distance. Studies that revealed the presence of premotor neurons that fire with respect to conjugate horizontal saccades in the pons and symmetric vergence movements in the midbrain provide support for the Hering model (for review[3,24]). Specifically, PPRF burst neurons and nPH tonic neurons provide horizontal saccade signals to abducens motoneurons that move the ipsilateral eye and to abducens internuclear neurons that project to the medial rectus subdivisions of the oculomotor nucleus to move the contralateral eye. Midbrain near response neurons supply medial rectus motoneurons with convergence signals and abducens motoneurons with divergence signals. These recording studies were supported by electrical stimulation studies that showed conjugate horizontal movements with activation of the PPRF, and vergence movements with activation of the midbrain near response regions dorsal and lateral to III.[6,25,26] Modern versions of the Hering model that incorporated the details of these neurophysiologic investigations have been developed by Zee and colleagues[27] and by Mays.[28]

In contrast, evidence in support of the Helmholtz model has come from experiments that used a variation on the Müller paradigm and by comparing the number of spikes generated for matched conjugate and disjunctive saccades. These studies indicate that the majority of neurons in the PPRF and nPH are actually uniocular, that is, most of their firing is related to changes in the position of one eye, not the other.[4,29,30–32] A similar pattern was observed within the motoneurons and the internuclear neurons of the abducens nucleus.[4,33] Particularly noteworthy is the finding that premotor neurons in the PPRF modulate their firing with respect to eye position during vertical vergence,[34] because it suggests that this region is not just involved in conjugate horizontal gaze. Based on these findings, modern versions of the Helmholtz model have been developed that indicate that

Investigative Ophthalmology & Visual Science

the control of vergence angle during disjunctive saccades is primarily derived from the horizontal gaze centers in the PPRF and nPH.[5,35]

At present, both of these models fail to explain all of the findings associated with disjunctive saccades. Neither fully explains why disjunctive saccades are slower than conjugate saccades, but considerably faster than symmetric vergence movements,[36–38] although attempts have been made in this regard.[39] Most of the tonically firing, midbrain near response neurons that supply vergence angle signals are silent during conjugate saccades[16,21], and their activity is not enhanced appropriately during disjunctive saccades,[40] so they could not contribute to the faster vergence component of disjunctive saccades. Moreover, the Hering models do not explain the need for uniocular neurons in the horizontal gaze center, and the Helmholtz models do not explain the need for vergence burst neurons in the midbrain. The role of abducens internuclear neurons is particularly problematic for the Helmholtz model. When discovered, these cells were put forward as the anatomic substrate for conjugate horizontal movements of the contralateral eye.[41] If the ipsi eye and contra eye PPRF excitatory burst neurons and nPH tonic position neurons fed into homogeneous populations of ipsi eye motoneurons and contra eye internuclear neurons in the abducens nucleus, this would provide the perfect drive for disjunctive saccades. However, a relatively small portion of abducens internuclear neurons display firing that correlates with horizontal movements of the contralateral eye, and only one-half of the abducens motoneurons display activity that correlates primarily with the ipsilateral eye.[33] Moreover, other studies of abducens internuclear neuron firing suggest they are poorly suited to directing vergence activity in medial rectus motoneurons.[42,43]

Lens accommodation latency is decreased and speed is increased during disjunctive saccades,[44] but it is not clear how this might be accomplished using the Helmholtz models centered on the PPRF and nPH. Indeed, premotor neurons were not found at pontine levels in either the present ciliary muscle injection experiments or previous ones done with conventional rabies virus.[8,9] So the premotor control of at least the lens accommodation component of the near response likely takes place at midbrain levels. It has been suggested that introducing the cMRF into the circuitry for controlling disjunctive saccades may be helpful in this regard.[9,13] The cMRF is known to be involved in horizontal gaze.[45–47] Moreover, neurons with uniocular patterns of firing have been found in the cMRF and stimulation of the cMRF can lead to disjunctive saccades.[22] Finally, the cMRF premotor neurons provide input to the ipsilateral medial rectus singly innervated fiber motoneurons,[13] so they are in a position to independently control the line of sight of each eye during disjunctive saccades. The present findings suggest that cMRF cells might also produce faster accommodation during these eye movements.

Our experiment explored the laterality of the premotor population that controls lens accommodation. We found evidence for both binocular and uniocular control of lens accommodation. Most of the premotor neurons in the SOA and in the cMRF were doubly labeled, indicating that they projected to both EWpg nuclei and that they controlled focus in both eyes. This would yoke the activity of the ciliary muscle in the two eyes, as predicted by the Hering models. Modern monocular models[5,30,35] also indicate that slow, symmetric vergence is bilaterally controlled by cells in the SOA. Indeed, lens accommodation in the two eyes is generally closely matched,[48,49] and when one eye is covered, its degree of accommodation still matches that of the viewing eye.[50] In line with the tight coupling of vergence and accommodation,[51] 25% to 50% of near response neurons encode both lens accommodation and vergence.[6,7] Thus, it seems highly likely that many convergence cells project bilaterally to both the medial rectus and EWpg motoneuron populations. Certainly, premotor neurons are found bilaterally in SOA and the cMRF after unilateral rabies injections of the medial rectus muscle in guinea pigs, even though this species is lateral eyed.[11]

A smaller subset of neurons in the SOA and cMRF projected either ipsilaterally or contralaterally to EWpg. This finding is supported by an antidromic testing study of SOA near response neurons encoding vergence and lens accommodation, which indicated that these cells projected to the ipsilateral oculomotor nucleus.[7] The presence of unilateral populations is also supported by recordings in the cMRF that indicated the presence of uniocular neurons with saccade-related activity.[22] Working in tandem, the ipsi- and contralaterally projecting EWpg premotor populations would have the same effect as the bilaterally projecting population. However, working in isolation, these populations could change the focus in one eye relative to the focus in the other eye, a pattern predicted by the Helmholtz model. The ability to individually control focus in each eye is limited (±1.0 D), but present.[52] This capability may supplement isometropization during development, allowing feedback control of lens accommodation to adapt the control system for differences in lens accommodation between the two eyes. There is evidence that both the SOA and the cMRF are targeted by cerebellar inputs that could underlie such adaptation.[53,54] However, these uniocular EWpg premotor neurons may also allow each eye to separately focus on targets located close to the observer, near the edge of the horizontal field. In this case, the distance between each eye and the target would differ enough that different levels of accommodation would be necessary for clearly imaging the target on both retinae. Under such conditions, the yoked inputs would provide the drive to achieve most of the required lens accommodation, and the uniocular inputs would provide detailed adjustment to compensate for the difference between the two eyes. In essence, both Hering and Helmholtz type mechanisms would be present, and work in concert.

Acknowledgments

Without the support and assistance of the staff of the Systems Neuroscience Institute and the Center for Neuroanatomy and Neurotropic Diseases at the University of Pittsburgh Medical Center, and their Director, Peter Strick, PhD, this study would not have been possible. In particular, we thank Isabelle Billig, PhD, who developed this recombinant rabies technique, for her extremely knowledgeable input. We are grateful for the gifts of recombinant rabies viruses and antibody to the rabies virus supplied by Christoph Wirblich and Matthias Schnell of Thomas Jefferson University that were absolutely critical to this work. We also thank Jinrong Wei for undertaking the immunohistochemistry and for her help with the illustrations.

Supported by a grant from the National Institutes of Health, EY014263, to Paul J. May and Paul D. Gamlin, and P30 EY03039 to UAB.

Disclosure: **P.J. May,** None; **P.D. Gamlin,** AGTC (F), Editas Medicine (F), Lacerta Therapeutics (F), AAVANTIBio (F)

Investigative Ophthalmology & Visual Science

References

1. Hering E. *The Theory of Binocular Vision*. 1868, Edited and translated by Bridgeman B, Stark L (Eds.). New York, NY: Plenum Press; 1977.
2. Helmholtz H. *Treatise on Physiological Optics*. 1910, Edited and translated by Southall JPC (Ed.). New York, NY: Dover Press; 1924.
3. Hepp K, Henn V, Vilis T, Cohen B. Brainstem regions related to saccade generation. In: Wurtz RH, Goldberg ME, (Eds). *The Neurobiology of Saccadic Eye Movements*. Rev Oculomotor Res, Vol 3. Amsterdam, the Netherlands: Elsevier; 1989:105–201.
4. Zhou W, King WM. Premotor commands encode monocular eye movements. *Nature*. 1998;393:692–695.
5. King WM. Binocular coordination of eye movements: Hering's Law of equal innervation or uniocular control? *Eur J Neurosci*. 2011;33:2139–2146.
6. Judge SJ, Cumming BG. Neurons in the monkey midbrain with activity related to vergence eye movement and accommodation. *J Neurophysiol*. 1986;55:915–930.
7. Zhang Y, Mays LE, Gamlin PD. Characteristics of near response cells projecting to the oculomotor nucleus. *J Neurophysiol*. 1992;67:944–960.
8. May PJ, Warren S, Gamlin PDR, Billig I. An anatomic characterization of the midbrain near response neurons in the macaque monkey. *Invest Ophthalmol Vis Sci*. 2018;59:1486–1502.
9. May PJ, Billig I, Gamlin PD, Quinet J. Central mesencephalic reticular formation control of the near response: lens accommodation circuits. *J Neurophysiol*. 2019;121:1692–1703.
10. May PJ, Warren S, Bohlen MO, Barnerssoi M, Horn AK. A central mesencephalic reticular formation projection to the Edinger-Westphal nuclei. *Brain Struct Funct*. 2016;221:4073–4089.
11. Graf W, Gerrits N, Yatim-Dhiba N, Ugolini G. Mapping the oculomotor system: the power of transneuronal labelling with rabies virus. *Eur J Neurosci*. 2002;15:1557–1562.
12. Ugolini G, Klam F, Doldan Dans M, et al. Horizontal eye movement networks in primates as revealed by retrograde transneuronal transfer of rabies virus: differences in monosynaptic input to "slow" and "fast" abducens motoneurons. *J Comp Neurol*. 2006;498:762–785.
13. Bohlen MO, Warren S, May PJ. A central mesencephalic reticular formation projection to medial rectus motoneurons supplying singly and multiply innervated extraocular muscle fibers. *J Comp Neurol*. 2017;525:2000–2018.
14. Billig I, Balaban CD. Zonal organization of the vestibulocerebellar pathways controlling the horizontal eye muscles using two recombinant strains of pseudorabies virus. *Neuroscience*. 2005;133:1047–1059.
15. Billig I, Strick PL. Anatomical evidence for shared control of eye and neck muscles by neurons in the ventral premotor cortex of a primate. *Soc Neurosci Abstr*. 2015;417.06.
16. Mays LE. Neural control of vergence eye movements: convergence and divergence neurons in midbrain. *J Neurophysiol*. 1984;51:1091–1108.
17. Das VE. Cells in the supraoculomotor area in monkeys with strabismus show activity related to the strabismus angle. *Ann N Y Acad Sci*. 2011;1233:85–90.
18. Das VE. Responses of cells in the midbrain near-response area in monkeys with strabismus. *Invest Ophthalmol Vis Sci*. 2012;53:3858–3864.
19. Pallus A, Walton MMG, Mustari M. Activity of near-response cells during disconjugate saccades in strabismic monkeys. *J Neurophysiol*. 2018;120:2282–2295.
20. Bohlen MO, Warren S, May PJ. A central mesencephalic reticular formation projection to the supraoculomotor area in macaque monkeys. *Brain Struct Funct*. 2016;221:2209–2229.
21. Mays LE, Porter JD, Gamlin PD, Tello CA. Neural control of vergence eye movements: neurons encoding vergence velocity. *J Neurophysiol*. 1986;56:1007–1021.
22. Waitzman DM, Van Horn MR, Cullen KE. Neuronal evidence for individual eye control in the primate cMRF. *Prog Brain Res*. 2008;171:143–150.
23. Quinet J, Schultz K, May PJ, Gamlin PD. Are there distinct roles for SOA and cMRF premotor neurons in disconjugate eye movements in the primate? *Soc Neurosci Abst*. 2017;150.06.
24. Büttner U, Büttner-Ennever JA. Present concepts of oculomotor organization. *Prog Brain Res*. 2006;151:1–42.
25. Bender MB, Shanzer S. Oculomotor pathways defined by electrical stimulation and lesions in the brainstem of the monkey. In: Bender MB, ed. *The Oculomotor System*. New York, NY: Harper & Row: 1964;81–144.
26. Cohen B, Komatsuzaki A. Eye movements induced by stimulation of the pontine reticular formation: evidence for integration in oculomotor pathways. *Exp Neurol*. 1972;36:101–117.
27. Zee DS, Fitzgibbon EJ, Optican LM. Saccade-vergence interactions in humans. *J Neurophysiol*. 1992;68:1624–1641.
28. Mays LE. The neural control of vergence eye movements. In: Chalupa LM, Werner JS , (Eds.). *The Visual Neurosciences*. Cambridge, MA: MIT Press; 2004:1415–1427.
29. Zhou W, King WM. Ocular selectivity of units in oculomotor pathways. *Ann N Y Acad Sci*. 1996;781:724–728.
30. King WM, Zhou W. New ideas about binocular coordination of eye movements: is there a chameleon in the primate family tree? *Anat Rec*. 2000;261:153–161.
31. Sylvestre PA, Choi JT, Cullen KE. Discharge dynamics of oculomotor neural integrator neurons during conjugate and disjunctive saccades and fixation. *J Neurophysiol*. 2003;90:739–754.
32. Van Horn MR, Sylvestre PA, Cullen KE. The brain stem saccadic burst generator encodes gaze in three-dimensional space. *J Neurophysiol*. 2008;99:2602–2616.
33. Sylvestre PA, Cullen KE. Dynamics of abducens nucleus neuron discharges during disjunctive saccades. *J Neurophysiol*. 2002;88:3452–3468.
34. Van Horn MR, Cullen KE. Dynamic coding of vertical facilitated vergence by premotor saccadic burst neurons. *J Neurophysiol*. 2008;100:1967–1982.
35. Cullen KE, Van Horn MR. The neural control of fast vs. slow vergence eye movements. *Eur J Neurosci*. 2011;33:2147–2154.
36. Enright JT. Changes in vergence mediated by saccades. *J Physiol*. 1984:350:9–31.
37. Enright JT. The remarkable saccades of asymmetrical vergence. *Vision Res*. 1992;32:2261–2276.
38. Maxwell JS1, King WM. Dynamics and efficacy of saccade-facilitated vergence eye movements in monkeys. *J Neurophysiol*. 1992;68:1248–1260.
39. Busettini C, Mays LE. Saccade-vergence interactions in macaques. II. Vergence enhancement as the product of a local feedback vergence motor error and a weighted saccadic burst. *J Neurophysiol*. 2005;94:2312–2330.
40. Pallus AC, Walton MMG, Mustari MJ. Response of supraoculomotor area neurons during combined saccade-vergence movements. *J Neurophysiol*. 2018;19:585–596.
41. Highstein SM, Baker R. Excitatory termination of abducens internuclear neurons on medial rectus motoneurons: relationship to syndrome of internuclear ophthalmoplegia. *J Neurophysiol*. 1978;41:1647–1661.

Investigative Ophthalmology & Visual Science

42. Gamlin PD, Gnadt JW, Mays LE. Abducens internuclear neurons carry an inappropriate signal for ocular convergence. *J Neurophysiol*. 1989;62:70–81.
43. Miller JM, Davison RC, Gamlin PD. Motor nucleus activity fails to predict extraocular muscle forces in ocular convergence. *J Neurophysiol*. 2011;105:2863–2873.
44. Schor CM, Lott LA, Pope D, Graham AD. Saccades reduce latency and increase velocity of ocular accommodation. *Vision Res*. 1999;39:3769–3795.
45. Cohen B, Waitzman DM, Büttner-Ennever JA, Matsuo V. Horizontal saccades and the central mesencephalic reticular formation. *Prog Brain Res*. 1986;64:243–256.
46. Waitzman DM, Silakov VL, Cohen B. Central mesencephalic reticular formation (cMRF) neurons discharging before and during eye movements. *J Neurophysiol*. 1996;75:1546–1572.
47. Waitzman DM, Silakov VL, DePalma-Bowles S, Ayers AS. Effects of reversible inactivation of the primate mesencephalic reticular formation. I. Hypermetric goal-directed saccades. *J Neurophysiol*. 2000;83:2260–2284.
48. Campbell FW. Correlation of accommodation between the two eyes. *J Opt Soc Am*. 1960;50:738.
49. Fisher SK, Ciuffreda KJ, Hammer S. Interocular equality of tonic accommodation and consensuality of accommodative hysteresis. *Ophthalmic Physiol Opt*. 1987;7:17–20.
50. Ball EA. A study of consensual accommodation. *Am J Optom Arch Am Acad Optom*. 1952;29:561–574.
51. Maxwell J, Tong J, Schor CM. The first and second order dynamics of accommodative convergence and disparity convergence. *Vision Res*. 2010;50:1728–1739.
52. Marran L, Schor CM. Lens induced aniso-accommodation. *Vision Res*. 1998;38:3601–3619.
53. May PJ, Porter JD, Gamlin PD. Interconnections between the primate cerebellum and midbrain near-response regions. *J Comp Neurol*. 1992;315:98–116.
54. Bohlen MO, Warren S, Moreno P, May PJ. Does the fastigial nucleus project directly to oculomotor motoneurons? *Soc Neurosci Abst*. 2013;363.04.

Investigative Ophthalmology & Visual Science